Local Electroporation of Single Adherent Cells by Micro-Structured Needle Electrodes

Kiran K. Sriperumbudur[1], Philipp J. Koester[1], Marco Stubbe[1], Carsten Tautorat[1], Jochen Held[2], Werner Baumann[1] and Jan Gimsa[1]*
[1]University of Rostock, Chair of Biophysics, Gertrudenstr. 11a, 18057 Rostock, Germany
[2]Microsystem Material Laboratory, Department of Microsystems Engineering (IMTEK), University of Freiburg, Germany
*Corresponding author: jan.gimsa @uni-rostock.de

Abstract: In spite of its low throughput, Patch-Clamp is the established method for intracellular measurements of the transmembrane potential. To address this problem, we have developed new biosensor-chips with micro-structured needle electrodes (MNEs). MNE-penetration of single cells growing on the MNE-tips leads to a situation comparable to the whole-cell mode in classical Patch Clamp. MNE-penetration was accomplished by local micro-invasive needle electroporation (LOMINE; Koester et al., 2008; Baumann et al., 1998a and b). In this paper, we simulate the field and potential distributions around the MNE before LOMINE assuming reasonable cell and medium parameters for a cell being in contact with the needle via focal adhesion points.

Keywords: Patch-Clamp, biosensor-chips, numerical simulation, COMSOL, induced transmembrane voltage

1. Introduction

Usually, the whole-cell mode with the classical Patch-Clamp is time consuming and automation is desirable. First automated methods have been developed for suspended cells (Farre et al., 2009; Stett et al., 2003). Nevertheless, most of the cells in the human body grow adherently. Therefore, new biosensor-chip systems are required to tackle the problem of Patch-Clamp of adherently growing cells.

1.1 New Biosensor-chips

We have developed new biosensor-chip structures to patch adherently growing cells. Our chips have 64 micro-structured needle electrodes (MNE) within a measuring area of 1 mm^2 (Fig. 1).

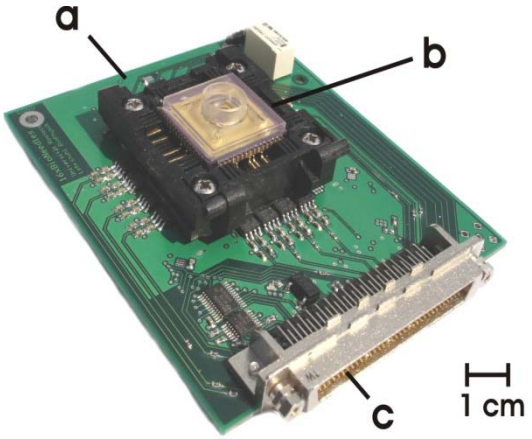

Fig. 1: (a) Removable chip socket (b) Biosensor-chip (c) Interface to data acquisition card

1.2 Micro-structured needle electrodes (MNE)

Three steps dry etching processes (isotropic-anisotropic-isotropic) have been used for producing either solid or hollow MNEs on a silicon base (Held et al., 2008). The MNEs are arranged in an 8×8 microelectrode array on the biosensor-chip (Fig. 2).

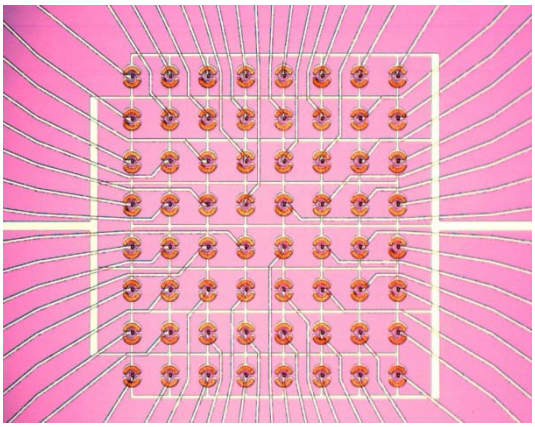

Fig. 2 (a): 8×8 MNE array in Biosensor-chip

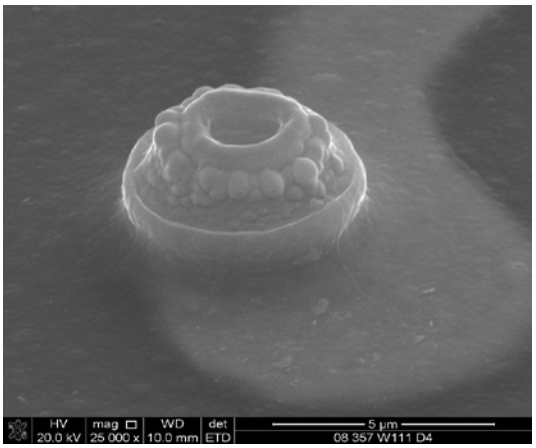

Fig. 2 (b): Scanning Electron Microscope (SEM) image of hollow MNE

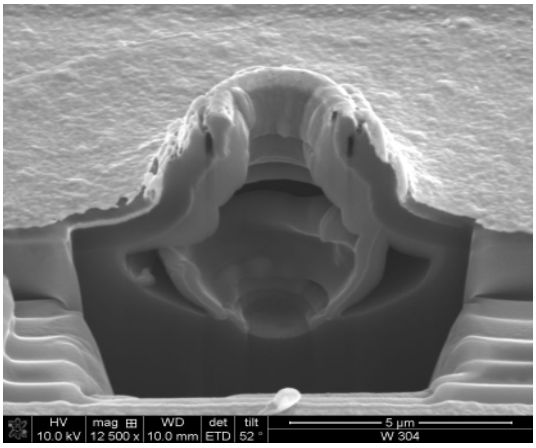

Fig. 2 (c): FIB cut of hollow MNE

2. Method

When cells are seeded on a sensor chip, they are more or less homogeneously distributed on the surface of the chip. Dielectrophoretic cell allocation has been applied either to the MNEs or to additional dielectrophoretic electrodes to increase the yield of cells growing on top of the MNEs (Gimsa and Wachner 1998, Prasad et al., 2003). The LOMINE-method (Fig. 3) was applied after L929 mouse tumor fibroblasts were cultured for one day and cell confluence was reached.

In classical electroporation, a very high electric field induces a high trans-membrane voltage, leading to the formation of membrane pores at both pole areas of the cell (Maswiwat et al., 2007). In LOMINE, the lipid membrane experiences a very high local electric field at the tip of the MNE, resulting in local electro-pores in the nanometer range (Fig. 4).

The success of LOMINE depends on the electric pulse characteristics (shape, length and repetition rate). Membrane penetration by the MNE is vital for detecting the transmembrane potential. Due to strong interaction between the electroporation pulses and the lipid membrane, the single phospholipids are disassembling and the cytoplasm gets into contact with the MNE metal or the MNE hollow core. These electrodes were able to detect the intracellular potentials for several minutes before they were poisoned by electrochemical processes.

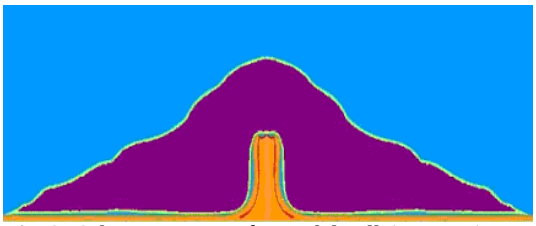

Fig. 3: Schematic view of a model-cell (magenta) on a solid silicon (orange) MNE with a platinum cover layer (red) before LOMINE. Light blue: cell culture medium; pale white: cell membrane. Solid silicon MNEs are not used in modeling.

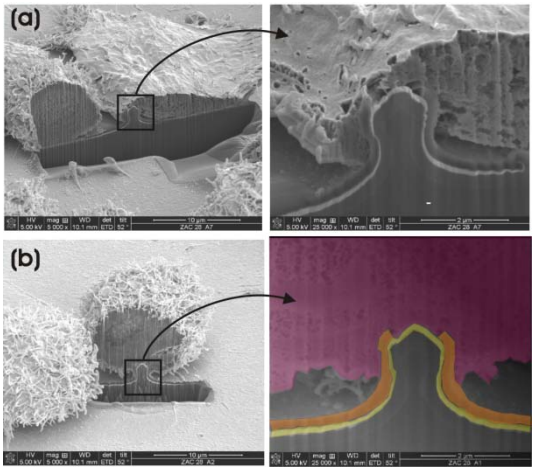

Fig. 4: SEM pictures of Focused Ion Beam (FIB) cuts of electroporated L929 mouse sarcoma fibroblasts overgrowing a solid MNE after electroporation. (a) Membrane penetration by LOMINE. Cells are vital for at least 1 day after LOMINE. (b) Digitally stained L929 cell. Magenta: fibroblast; orange: Si_3N_4-passivation; yellow: MNE tip metallization. FIB cuts are accomplished according to the protocol of Heilmann et al., 2007.

3. Model

The COMSOL multiphysics AC/DC module was applied to a 2D axial symmetric model. The model has five subdomains (Fig. 5). The red area represents the hollow platinum needle. The Si_3N_4 insulation, the intra- and extracellular media are orange, magenta and blue, respectively. The pale white thin circumference of the magenta area represents the membrane. The hollow portion of the needle is dark blue. Reasonable boundary conditions and the following subdomain material properties were assumed and solved in the quasi-electrostatic mode.

Subdomain	**Electric conductivity (σ) in S/m**	**Relative permittivity (ε_r)**
External medium	1.4	70
Internal medium	0.3	60
Membrane (8 nm)	1×10^{-6}	15
Platinum MNE	9.52×10^{6}	1
Passivation (Si_3N_4)	0	9.7

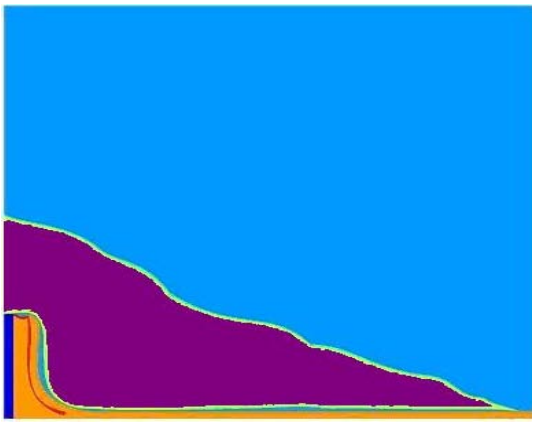

Fig. 5: Subdomain plot of the model.

4. Results

Fig. 6 and Fig. 7 present the solution. The electric field streamlines show the high field intensity at the tip of the MNE confirming the high possibility of LOMINE. Fig. 4 and Fig. 8 present the supporting laboratory results of the successful LOMINE of L292 mouse sarcoma fibroblasts overgrowing a solid and hollow MNE, respectively.

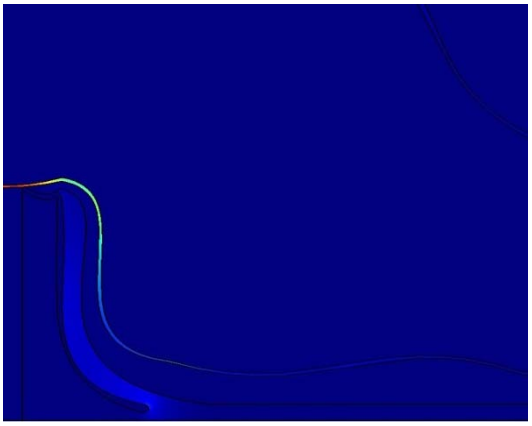

Fig. 6 Field intensity plot (color-coded). High electric field intensities are observed in the membrane and at the tip of the MNE.

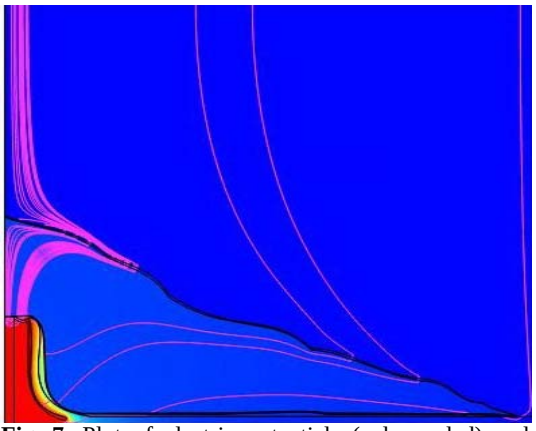

Fig. 7: Plot of electric potentials (color-coded) and field line orientation (pink) as obtained from COMSOL for a frequency of 200 kHz.

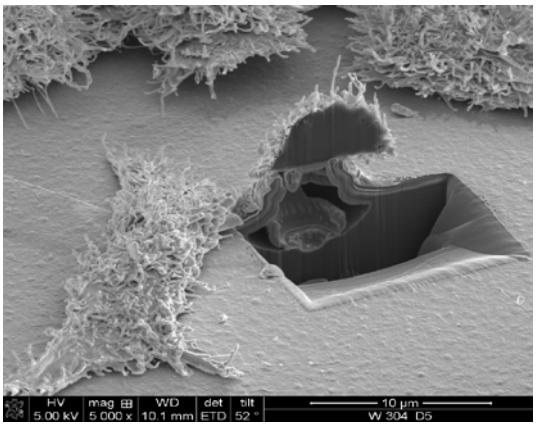

Fig. 8: FIB cut of an attached L929 cell after LOMINE by a hollow MNE.

5. Conclusion

For the cell model, we considered a body of revolution with an arbitrary circumference line, even though the biological cells exhibited an arbitrary shape. This simplified assumption allowed us to use a model with a 2D axial symmetry and an easier solution of the problem. The observations and results of this simulation will be compared to the practical laboratory results to further optimize MNE structures and LOMINE parameters.

6. References

1. Baumann W., R. Ehret, M. Lehmann, G. Igel, H.-J. Gahle, B. Wolf, U. Sieben, I. Freund, and M. Brischwein. Verfahren und Vorrichtung zur Messung eines Zellpotentiales. Patent DE 19827957, EP 960933, US 6368851, JP 11346794(1998a)
2. Baumann W., R. Ehret, M. Lehmann, G. Igel, H.-J. Gahle, B. Wolf, U. Sieben, I. Freund, and M. Brischwein. Verfahren und Vorrichtung zur intrazellulären Manipulation einer biologischen Zelle. Patent DE 19841337, EP 962524A1, US 6475760, JP 11346794(1998b)
3. Farre C., A. Haythornthwaite, S. Stoelzle, M. Kreir, M. George, A. Brueggemann, and N. Fertig. Port-a-patch and patchliner: high fidelity electrophysiology for secondary screening and safety pharmacology. *COMB CHEM HIGH T SCR* **12**:24-37 (2009)
4. Gimsa J. and D.Wachner. A unified resistor-capacitor model for impedance, dielectrophoresis, electrorotation and induced transmembrane potential. *Biophys J* **75**, 1107–1116 (1998)
5. Heilmann A., F. Altmann, A. Cismak, W. Baumann, and M. Lehmann. Investigation of cell-sensor hybrid structures by Focused Ion Beam (FIB) technology, *mrs proceedings*, 0983-LL03-03 (2007)
6. Held J., J. Gaspar, P.J. Koester, C. Tautorat, A. Cismak, W. Baumann, A. Trautmann, P. Ruther, and O. Paul. Microneedle arrays for intracellular recording applications. *In: IEEE MEMS congress proceedings*, Tucson, USA, 268-271 (2008)
7. Koester P.J., C. Tautorat, A. Podssun, J. Gimsa, L. Jonas, and W. Baumann. A new principle for intracellular potential measurements of adherently growing cells. *In: 6th international meeting on substrate-integrated micro electrode arrays*, Reutlingen, Germany, ISBN 3-938345-05-5 274-277 (2008)
8. Maswiwat K, D. Wachnner, R. Wanke, and J. Gimsa. Simplified equations for the transmembrane potential induced in ellipsoidal cells rotational symmetry. *Phys J* D: Appl Phys **40** 914-923 (2007)
9. Prasad S., M. Yang, X. Zhang, C. S. Ozkan, and M. Ozkan. Electric field assisted patterning of neuronal networks for the study of brain functions, *Biomed Microdevices* **5**:125-137 (2003)
10. Stett A., C. Burckhardt, U. Weber, P. van Stiphout, and T. Knott. CYTOCENTERING: A novel technique enabling automated cell-by-cell patch clamping with the CYTOPATCH chip. *Receptor Channel* **9**:59-66 (2003)